

# Explainable AI for Engineering Design: A Unified Approach of Systems Engineering and Component-Based Deep Learning<sup>1</sup>

Philipp Geyer<sup>2</sup>, Manav Mahan Singh<sup>3</sup>, Xia Chen<sup>2</sup>

**Abstract**—Data-driven models created by machine learning gain in importance in all fields of design and engineering. They have high potential to assist decision-makers in creating novel artefacts with better performance and sustainability. However, limited generalization and the black-box nature of these models lead to limited explainability and reusability. To overcome this situation, we propose a component-based approach to create partial component models by machine learning (ML). This component-based approach aligns deep learning with systems engineering (SE). The key contribution of the component-based method is that activations at interfaces between the components are interpretable engineering quantities. In this way, the hierarchical component system forms a deep neural network (DNN) that a priori integrates information for engineering explainability. The large range of possible configurations in composing components allows the examination of novel unseen design cases outside training data. The matching of parameter ranges of components by similar probability distribution produces reusable, well-generalizing, and trustworthy models. The approach adapts the model structure to engineering methods of systems engineering and to domain knowledge. We examine the performance of the approach by the field of energy-efficient building design: First, we observed better generalization of the component-based method by analyzing prediction accuracy outside the training data. Especially for representative designs different in structure, we observe a much higher accuracy ( $R^2 = 0.94$ ) compared to conventional monolithic methods ( $R^2 = 0.71$ ). Second, we illustrate explainability by exemplary demonstrating how sensitivity information from SE and rules from low-depth decision trees serve engineering. Third, we evaluate explainability by qualitative and quantitative methods demonstrating the matching of preliminary knowledge and data-driven derived strategies and show correctness of activations at component interfaces compared to white-box simulation results (envelope components:  $R^2 = 0.92..0.99$ ; zones:  $R^2 = 0.78..0.93$ ).

**Keywords:** Artificial intelligence, machine learning, regression model, systems engineering, complex systems, surrogate model

## 1 Introduction

### 1.1 Data-driven Prediction in Design and Engineering

Increasingly data-driven models provide assistance in complex engineering design tasks. The data-driven models are

meanwhile able to capture the complexities sufficiently. Moreover, the computational power required to create the models is not a limiting factor anymore. Due to this reason, there are many applications in engineering-related domains. The prediction of the energy demand of buildings [1–5] forms an important field because data-driven models avoid complex modelling and high computational load required for thermal simulations. Basically, these data-driven models are used as surrogates for simulations in sustainable building design [6, 7]. Following the same pattern, surrogate models for structural design and engineering have been created [8]. For dynamical systems, extreme learning with reduced training efforts has been established [9–11]. In fluid dynamics, data-driven modelling have been established for prediction of flows [12]. Furthermore, in operations research and systems engineering for control and decision problems including the analysis of dynamic systems deep learning methods got attention, recently [13].

The energy-efficient building domain with the dynamic complex thermal system will serve as an exemplary domain representing schemes analogously occurring in other domains of design and engineering. Designers and engineers developing a well-performing solution of such a system need feedback in real-time in a process called design space exploration (DSE) to understand how to improve a given design configuration [14]. This exploration process includes variation of a design configuration as a key technique to answer what-if questions. As this process requires analysis of many variants to gain this information, the use of physical simulations causes significant modelling and computation load. This load is substantial for real-time application in case physical simulation is used, which vitally limits the exploration process. This opens up opportunities of design optimization as e.g. demonstrated in the context of green building design [15, 16]. Not only designing requires evaluation of many variants and states but also building energy classification, clustering and retrofit strategy development [17, 18] as well as control and management problems [19–21]. In this situation, data-driven modelling

<sup>1</sup> This work has been submitted to Advanced Engineering Informatics on 9 May 2024 for potential publication. Copyright may be transferred without notice.

<sup>2</sup> Sustainable Building Systems Group, Institute of Design and Construction, Leibniz University Hannover, geyer@iek.uni-hannover.de

<sup>3</sup> Georg Nemetschek Institute Artificial Intelligence for the Built World, Technical University of Munich

trained either on simulation results or on data collected from existing artefacts are applied as a highly interesting alternative to physical simulations.

### 1.2 Limitation of conventional ML and Contribution of CBML

However, there are two major limitations of current data-driven approaches for their application in engineering design:

- (1) **Generalization:** Data-driven models are only reliable within the distribution of the training dataset and often show a limited generalization. However, according to nature of design and engineering creating novel artefacts, there is the need for robust models with a good generalization. Decision makers need to be sure that models predict correctly in unseen cases different from the training data. Most application cases mentioned above vary parameters without changing the model structure—an approach we call monolithic model. This parametric monolithic approach allows to treat generalization as a statistical of input parameters identifying model boundaries. However, a pure parametric model is also limited in generalization significantly, as novel design cases frequently have different structures that cannot be covered with parametric changes; as a consequence, adaptation of the features of the data-driven model stays incomplete leading to inaccurate predictions. Slight mitigation provides the use of characteristic numbers instead of direct use of design parameters [22]—a best practice serving as benchmark in Section 3.
- (2) **Explainability:** Furthermore, designers and engineers need insights in how the models predict to check for plausibility, approve and justify results as well as to gain understanding of the behavior of the design configuration and the nature of the design space. This need calls for explainability of data-driven models. To address the shortcomings of the black-box character of ML models, a lot of research has been carried out addressing explainability [23]. On the one hand, there is a limited set of transparent models that are *interpretable* by humans. On the other hand, a huge set of *post-hoc methods* adds explainability to ML black-box models. LIME and SHAP as important post-hoc methods have also been transferred to building energy in several cases [24]. However, our experiments have shown that accessing activations in conventional deep neural network (DNN) directly as well as using SHAP delivers limited explainability [25, 26]—therefore, direct model interpretability, i.e. readability of model contents by humans, is of eminent interest.

**Contribution of CBML:** In contrast to monolithic models, we propose *component-based machine learning (CBML)*, a

method that composes the model architecture for prediction individually following a systems engineering approach described in detail in Section 2. In contrast to existing systems engineering integrations of ML [27–30], CBML does not use a monolithic model but breaks the data-driven model down to the design components. Ontologies provide a background for such system decomposition, such as existing schemes [31–34]; such ontologies have been combined with ML especially in the energy context [35, 36]—however, data-driven models have not been organized according to the ontologies up to now.

As a consequence of this systems decomposition, modelling aligned with the design case allows for far broader range of configurations providing much better *generalization*, i.e. higher accuracy in design cases less similar to training data, as demonstrated in Section 3. By composition pretrained models and thus modifying the models architecture, CBML has some parallels with transfer learning [37, 38]; in case of the use of artificial neural networks, the model form a DNN. However, in contrast to transfer learning, the interfaces between components have engineering quantities with units and therefore provide interpretable information. This information enables natural *explainability* and understanding by designers and engineers. In case of the DNN, the activations of the network are interpretable as engineering quantities at the component interfaces. In Section 4, we will demonstrate these benefits in terms of explainability and evaluation techniques [39, 40] to explore further understanding of the design space.

## 2 CBML Methodology and its Evaluation

To improve both the generalizability and explainability, we propose a component-based approach that aligns data-driven modelling to design and engineering. We create data-driven models for the design and engineering process following a system engineering paradigm described by [41]. The decomposition according to this paradigm using system components with input and output parameters forming the interfaces between the components are the key elements of CBML; above mentioned ontologies served as background for the decomposition. This approach provides the basis for engineering interpretability and the reusability of components leading to broad generalization. Furthermore, it makes the data-driven models accessible to existing systems analysis methods, such as compiled by [42].

To construct the components, we used artificial neural networks (ANN) because of their high flexibility or capacity, although other ML modelling methods are possible, too. The data-driven model based on ANN methods forms by the components composition a DNN with one particularity: Besides the layer functions  $f_l$ , the component function  $f_c$  includes at the interfaces functions for scaling  $v$  and inverse scaling  $v^{-1}$  to provide the interpretable engineering quantities  $y_r$  with units:

$$f_c(\mathbf{x}) = \mathbf{y}_r = \nu^{-1} \left( f_l^n \left( \dots f_l^2 \left( f_l^1 \left( \nu(\mathbf{x}) \right) \right) \right) \right). \quad (1a)$$

This includes typical functions  $f_l$  for the inner ANN layers:

$$f_l(x) = \mathbf{y}_l = \sum_{i=1}^n \mathbf{w}^T \phi(\mathbf{x}) + w_0; \quad (1b)$$

where  $\phi$  is the activation function,  $\mathbf{x}$  are the input parameters, and  $\mathbf{w}$  and  $w_0$  are learning parameters.

As a consequence of the scaling and inverse scaling, during composition of the data-driven model for prediction, shown in Equation 1a, all inputs  $\mathbf{x}$  and outputs  $\mathbf{y}$  of a component are subject to engineering units. Therefore, the activations at interfaces between components have units of heat flow, heating and cooling demand, and final energy consumption in W or in kWh/a or in kWh/m<sup>2</sup>a in case of energy performance prediction. In this way, a DNN is created that allows direct interpretation of engineering quantities within the network.

During the training process, labeled training data for a supervised learning procedure are used at component level. These data form the training set  $X_c$  for each component  $c$  with  $n_c$  samples to connect the features  $\mathbf{x}_c$  with the labels  $\mathbf{y}_c$  to act as ground truth:

$$X_c = \{\mathbf{x}_c, \mathbf{y}_c\}_{n_c} \quad (2)$$

Training data have been collected from real world measurements [43] and synthetic data generated by state-of-the-art dynamic simulation tools [44, 45]. Training takes place in a supervised learning process component by component using the respective input and output data, as illustrated for window and wall components in Figure 1a. Given such labeled sets, standard training processes serve to adapt the component functions, e.g. by adapting the weight parameters  $\mathbf{w}$  and  $w_0$  in Equation 1 by a gradient-based method.

In case of prediction, the components are composed to represent the design artefact in its current configuration. By connecting inputs and outputs of the components to a system representing new designs, the data-driven models are reused for unseen configurations (Figure 1b). Aligning the component structure to the methods of digital modelling (in case of buildings: building information modelling, BIM [46]; industry foundation classes, IFC [29]) fosters automatic generation of the data-driven models.

Formally, in prediction, the system function  $f_s$  as a DNN is composed in  $h$  hierarchical levels with nested component functions  $f_c$  with  $n_h$  components at each level:

$$f_s(\mathbf{x}_s) = \hat{\mathbf{y}}_s = f_c^{h, n_h} \left( \dots \left( f_c^{2,1} \left( \begin{array}{c} f_c^{1,1}(\mathbf{x}_{l,1}) \\ \dots \\ f_c^{1,m}(\mathbf{x}_{l,m}) \end{array} \right) \right) \dots \left( f_c^{2,n_2} \left( \begin{array}{c} f_c^{1,m+1}(\mathbf{x}_{l,m+1}) \\ \dots \\ f_c^{1,n_1}(\mathbf{x}_{l,n_1}) \end{array} \right) \right) \right) \quad (3)$$

The validation takes place at the system level. For this purpose, a labeled validation dataset  $X_s$  with a variety of  $s$  structures, i.e. differing compositions of components, serve to examine performance for typical system structures. This set includes first the system topology as a directed acyclic graph  $G_s$  which includes the used components as nodes  $V_c$  and their connecting edges  $E_c$ ; second it includes the parametric features  $\mathbf{x}_s$  at system level with labels  $\mathbf{y}_s$  to act as ground truth for validation:

$$X_s = \{G_s, \mathbf{x}_s, \mathbf{y}_s\}_{n_s} \quad \text{with } G_s = \{V_c, E_c\} \quad (4)$$

On the basis, of  $G_s$  and  $\mathbf{x}_s$  the matrix in Equation **Error! Reference source not found.** is populated und delivers predictions  $\hat{\mathbf{y}}_s$  to be compared with the ground truth  $\mathbf{y}_s$  in the validation dataset  $X_s$ . This validation tells about the overall system prediction performance of the data-driven model.

This approach based on systems engineering and components provides a much wider generalization than the monolithic approach. The structure of data is met by selecting and composing the data-driven models as required to represent the design configuration. In the example, the monolithic model based on the training data shown in Figure 1a would only allow prediction for box buildings because of the structure of data and the model; The component-based approach allows prediction for a broad variety of design cases exemplified by the configurations shown in Figure 2, top. Because components occur in similar configuration in the novel design cases as they are present in the training dataset, the method avoids extrapolation, a serious problem for data-driven models. The grey boxes in Figure 1 (c-h) show examples of the matching of parameter ranges and distributions as histograms. There are parameter ranges, such as the u-value, which determines heat transmission through walls and windows, that can be configured directly and, thus, show a perfect match (Fig. 1d). Many other parameters depend on previously determined parameters and predictions so that no direct control is possible, but the match depends on other parameters of the design configuration. For instance, the wall area (Fig. 1c) depends on the building shape; heating and cooling loads (Fig. 1f,g) and the final energy demand (Fig. 1h) depend on dynamic thermal processes determined by component heat flows of the building envelope and zones parameters. Therefore, only an approximate

match is achievable. In general, all data show a good match for the example although the configuration of training and prediction is significantly different.

This demonstrates that CBML complies with two preconditions for use of data-driven models: (1) The structure of the model matches, i.e. parameters and their meaning coincide in training and prediction; (2) Parameter distribution in training cover distributions in prediction. In allowing this matching with varying model structure, CBML delivers a superior generalization with high flexibility. Appendices A and B describe the methodological details of the experimental data generation and the monolithic baseline model used as benchmark. Appendices C and D how to create the component-based models for single values and time series.

To summarize, the scheme to achieve this generalization

consists of the extraction of training data from one case, the encapsulation of component behavior as a data-driven model by ML, and the application by composition of data-driven models to the novel structures. This scheme is a form of inductive transfer learning (TL) [37] that is aligned to the engineering reasoning, to the underlying rules and, eventually, to the basic physical laws as a form of domain knowledge. The matching of the structure of the domain knowledge as well as that of probability distributions of features or parameters form important conditions of the transfer [38]. The component approach provides the basis for this inductive TL. We see it as a special class of inductive TL that extends data information by engineering knowledge consisting of the decomposition and re-composition of the artefact according to paradigm of systems engineering.

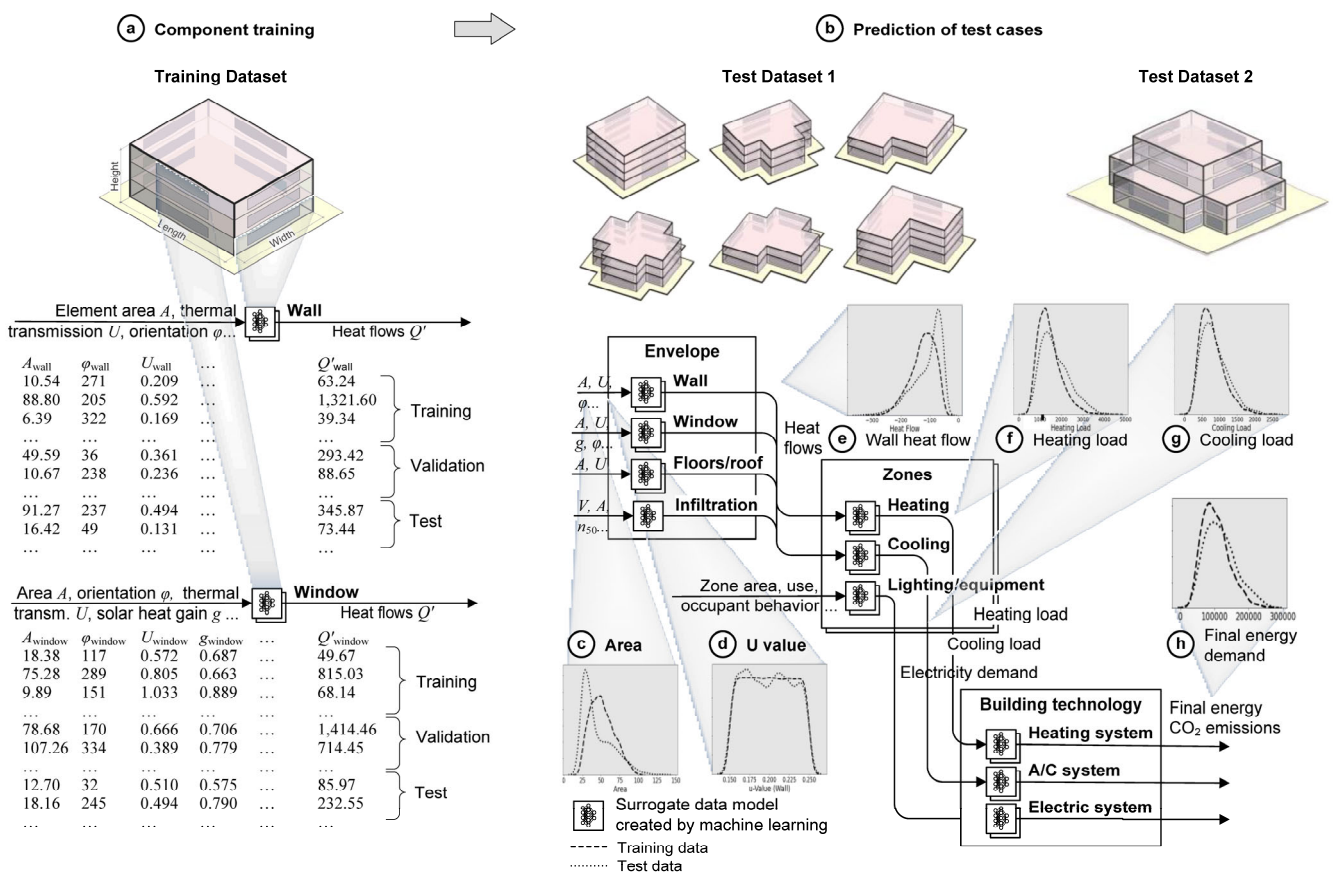


**Fig. 1. Component-based machine learning (CBML).** (a) Training takes place at component level. (b) For prediction of new cases, components are composed to new system configurations according to the structure of the design. This allows representing novel unseen configurations beyond training data based on domain knowledge. At the same time, it enables matching range and probability distribution of training data shown for exemplary parameters in the grey boxes (light dotted line: training data; thick dashed line: test data).

To evaluate the generalization capabilities, training and test datasets with different characteristics have been generated. The training process took place based on the simulation results from the box building shown in Figure 1a; details are described in Appendix A. Two test datasets with different structure of design

allow a realistic evaluation of generalization capabilities. Randomly generated design footprints form the first test set (Fig. 1b, Test Dataset 1). This set represents typical options in an early design phase of a building and includes a set of shapes that are different from the box building in the training data. As

a constraint of random generation, all storeys of the building have the same shape, which matches many real-world buildings. The second set (Fig. 1b, Test Dataset 2) is based on a designed building configuration whose complexity is higher because not all storeys have the same geometry; roofs occur at different levels, and the zone at level two is connected to roofs and a floor slab at the top. All generated models in training and test dataset are parametric in terms of geometry and engineering properties which reflects the design space at an early level of preliminary design. Section 3 provides results on generalization capabilities.

So, both test datasets contain additional complexity compared to the training data and serve to test the ML models for their ability to generalize beyond the training data. For the evaluation, the prediction of component-based ML models and of a monolithic model according to state-of-the-art as baseline method are compared. As the transfer between training and test datasets because of their models' different structure is not possible, the state-of-the-art uses geometric parameters or zone information not directly but performance-characterizing numbers valid for all buildings, such as floor area, height, number of floors, and relative compactness, following the methods of [22]; the use of such characteristic numbers currently delivers the best possible results for monolithic models in representing arbitrary design configurations (for details on the baseline method, see Appendix B).

For examining and demonstrating explainability, a common approach is the analysis of the activations and its propagation for a selected prediction case [47]. Layer-wise relevance propagation (LRP) [48] is a method used in image classification. Equivalently to DNN used in image analysis, the CBML structure forms, as mentioned, a DNN. To evaluate the capabilities of explainability, we compose prediction models for Test Dataset 2 according to the CBML method, which includes inverse scaling by the function  $v^{-1}$  at each interface and apply selected interpretation methods. First, looking at absolute quantities is straight forward. In Section 4.1, we show results on the interpretation of these quantities that enable engineers and designers to understand and check these results by domain knowledge. An alternative approach to examining activations directly is the local variation according to DSE and sensitivity analysis to gain information on reasons for prediction. We use this approach, which is a traditional engineering method to understand models' behavior and is closely related to local interpretable model explanation for classifiers (LIME) [49, 50]. It belongs to the model-agnostic post-hoc techniques of explainability [23]. From an engineering perspective, a linear local model built on DSE results delivers a linear regression coefficient that describes sensitivity and enables interpretation of the importance of parameters in the model. Sensitivity analysis as described by Menberg et al. [51] serves to generate the mean absolute mean  $\mu^*$  of the Elementary Effects (EE) with an  $\Delta_i$  of 5% (for Details see Appendix E). Section **Error!**

**Reference source not found.** provides exemplary sensitivities with explanations.

Another method to gain insights in reasons for prediction are local surrogate models. We use decision trees as local surrogate model, which form a post-hoc method of explainability [23]. Trees with low depth allow the extraction of rules that are understandable by engineers and provide further linking to domain knowledge. Appendix G describes methodological details on tree generation and results in Section 4.3 show exemplary derived rules.

Finally, we evaluate explainability by checking the properties of the CBML approach that offer the user insights and thus help to create trust. Schemes for evaluating explainability as developed by [23, 39, 40, 52] serve as background. Using the scheme of [40], first, we use a white box test evaluating information at component interfaces, examining explainability capabilities, and assuring correctness; Second, we check coherence with users' knowledge by evaluating statistics of interface values against design strategies as relevant domain knowledge. Section 0 shows the evaluation results.

### 2.1 Domain knowledge and its integration in CBML

Component-based ML is a way to align data-driven models with domain knowledge. In the case used in the paper, this knowledge deals with a focus on the complex dynamic thermodynamic processes between the building, its environment, and its control for a comfortable indoor environment with low energy demand. To enable readers who are not familiar with this domain knowledge to follow our methods, we provide a concise introduction in this paragraph. There are several key factors for an energy-efficient building. First, the area and the thermal insulation of walls, windows, roof and floor slab, the so-called u-value in  $W/m^2K$ , determine the heat flow from indoor the surrounding of the building. The envelope area of these elements, which is responsible for heat losses, strongly depends on the shape of the building. Therefore, the compactness i.e., the ratio of façade area to volume plays an important role and serves as an import characteristic number as mentioned before. Second the solar transmissivity of the windows, the so-called g-value determines how much heat energy the sun generates in the building, replacing heat from the building system in winter however causing cooling demand in summer. Heat capacity in  $J/kgK$  plays an important role in determining how much surplus heat is stored in building components and, thus, describing the dynamic interaction between solar gains, internal gains (heat emitted by users and devices), and heating and cooling systems. Given these dynamically interacting factors, it is complex and not trivial for designers and engineers to understand the thermodynamic behavior of a given design configuration and to find a well-performing solution.

The taxonomy of von Rden et al. [53] lists four entities in a

prototypical ML pipeline to integrate knowledge: training data, hypothesis set, learning algorithm, and final hypothesis. The focus of CBML is the integration of domain knowledge in the hypothesis set by the radical organization of the model architecture according to the domain knowledge and respective structures. In case of the example domain, i.e., energy-efficient building design, the structure originates from the system of the building including its services and constructions described in the mentioned domain ontologies. The domain-related model structure enables further connection to domain knowledge in the final hypothesis, i.e., the resulting predictions of CBML, and eventually generates explainability as discussed by [54]. A further source for knowledge embedded in components is the use of dynamic simulation to generate training data. By acquiring and using simulation results that are aligned to the component structure, CBML incorporates domain knowledge embedded in the complex system of the dynamic simulation model and its incorporated differential equations.

## 2.2 Domain characterization and method transfer

The paper provides evidence for the benefits of the CBML method by energy-efficient building design as test domain focusing on the thermodynamic behavior of buildings and the dynamics of its heating and cooling system. However, we expect that the method is transferable to other domains involving systems of similar characteristics. The following list aims to foster this transfer by explicitly describing the characteristics of the test domain:

- The test domain has partly linear or linearized and partly non-linear ordinary or partial differential equations (ODE/PDE) as well as differential algebraic equations (DAE) [55]. Simulation environments applied to these equation systems, such as the software EnergyPlus [56] used to generate data, involve the required solvers.
- The hierarchical nature of the system is a second characteristic of the test domain. Usually, the configuration of the building envelope determines the heat and cold demand of the zones. Heating and cooling systems perform dynamically depending on this demand. The organization as a data-driven system with such a unidirectional information flow cuts some of the dynamic feedback loops; however, our results show that this is less relevant than the missing adaptation to the specific design configuration enabled by the components.

Other domains dealing with systems have similar characteristics, which suggests the hypothesis of transferability of the method. Such examples are systems in electric circuits and respective control and power engineering problems with typically non-linear ODE and DAE [57], multibody mechanics that involve ODE and DAE [58] and structural engineering and dynamics [59]. Depending on the number and importance of

loops, we expect although not proven that CBML is applicable.

## 3 Results for Generalization

The quantitative results in terms of generalization tested by the set of random shapes demonstrate higher precision of the component-based method compared to the state-of-the-art monolithic method. The deviation of ML prediction from simulation results, which act as ground truth, show a mean absolute percentage error (MAPE) of only 3.76% and an  $R^2$  of 0.99 whereas the monolithic baseline model shows a MAPE of 5.88% and an  $R^2$  of 0.94 (Fig. 2a). The second set of design configurations adds more complexity, similar to what is usually present in realistic design and engineering cases of buildings. Under these conditions, the advantage of the component-based method against the monolithic method significantly increases. The MAPE of the component-based method is 4.96%, the  $R^2$  is 0.94 whereas the MAPE of the conventional method is 12.72% and the  $R^2$  is 0.71 (Fig. 2c). The monolithic model underestimates energy demand which is problematic from a domain perspective whereas component-based approach does not and is more precise (Fig. 2). This increase of difference for more complex cases is an indicator that the components show a much better ability to generalize typical design configurations of a domain instead of being linked to the behavior observable in the training dataset and the related case.

## 4 Results for Explainability

Using the derived data-driven model and the representative case based on Test Dataset 2 (Fig. 2c, d), we demonstrate in this section different approaches of explainability enabled by component-based ML. The first subsection deals with intrinsic explainability directly offered by the component interfaces in the system of the data-driven model. The second subsection deals with sensitivity analysis as a form of engineering interpretation for design space exploration (DSE) locally around an interesting configuration, which is the representative case shown in Figure 2d. The third subsection shows a decision tree as explainable surrogate model based on the local DSE data and derives engineering rules matching domain knowledge of design and engineering. In the final subsection, conclusions on explainability from these models are evaluated against domain knowledge.

### 4.1 Engineering insights in component systems

Figure 3 shows exemplary predictions at interfaces to illustrate how CBML model offers engineering insights offering explainability. The first example are predictions of yearly averages and totals (3a, e, h) and time series (3b, f) for wall heat flows, zone cooling load, and energy use intensity (EUI). The yearly numbers allow designers and engineers to

identify parts of the building causing high energy demand. For instance, the time series predictions (3b) show specific dynamic behavior allowing for understanding high demand, such as the heat flows through the East walls of the representative test case building. In July, the morning sun heats the wall up causing the peaks on each of the daily flows, e.g., indicating potential of thermal energy usage, whereas the medium level flows show conduction of heat from outside air to indoor space just causing cooling loads. Negative values show heat rejection through the walls in the night reducing cooling loads. Furthermore, the dynamic behavior of the cooling systems and total demand (3f, i) shows profiles caused by interaction of occupancy and system, such as internal gains and system shutdown on weekends. In cooling loads (3f), the consequent high peak after the weekend compared to the Friday before the weekend is predicted correctly; this is caused by the heating-up the building while the cooling system is turned off over the weekend.

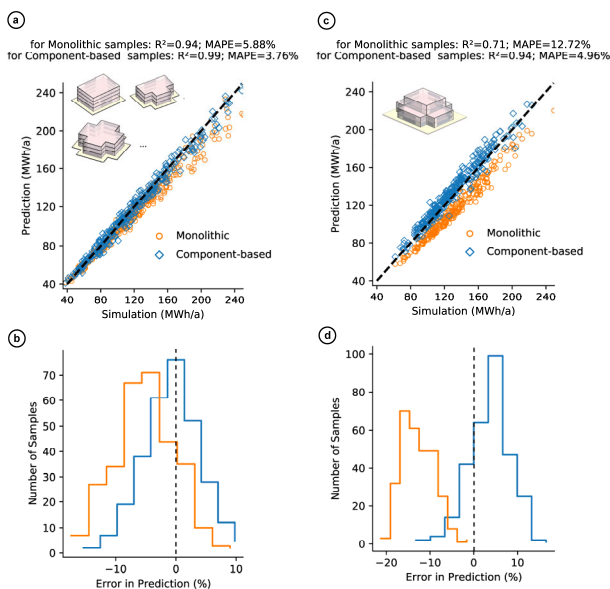


**Fig. 2. Prediction accuracy of test cases based on the ML components to evaluate generalization compared with state-of-the-art monolithic ML models.** The comparison of ML predictions by the component-based method and state-of-the-art monolithic to ground truth by simulation serves to examine generalization. (a), (b): Comparison of randomly generated shapes with all storeys same geometry as in the training data; (c), (d): More complex design configurations varied by engineering and geometry parameters. This configuration differs from the training data by a roof also at an intermediate level.

We would like to emphasize that all this information is gained from interpretable internal activations of a DNN formed by the component system. Although pure activations of a DNN prediction, this information provides explainability that allows domain experts to understand processes, to check results for plausibility, and to evaluate and modify the current design anticipating improved behavior. Furthermore, using not only one configuration but comparing and analyzing multiple

configurations, such as given by sensitivities (Fig 3b, f, i) and decision trees Fig 3d, provides further information for DSE; Subsection **Error! Reference source not found.** demonstrates sensitivities in detail whereas Subsection 4.3 deals with trees and derived rules.

#### 4.2 Local model explanation by sensitivity analysis

Figure 4 shows selected sensitivities for the representative test case in details. First, the matrix shows high sensitivities of the South wall and window heat flow for length and height of the building. A change of these parameters from  $\pm 5\%$  leads to about  $100 W_{avg}$  additional heat loss but about  $300 W_{avg}$  additional heat gains through the windows (Fig. 4a). This tells domain experts that the South windows are worth for looking for heat gains and energy savings. However, to understand the real potential one needs to know whether these heat gains occur in summer or winter. Looking at the g-value, also called solar heat gain coefficient, provides an answer (Fig. 4b): A change of the g-value increases heat gains by  $400 W_{avg}$ ; it reduces heating load by  $380 W_{avg}$  and total operational energy by  $250 kWh/a$ ; However, it increases cooling loads by  $370 W_{avg}$ . These observations tell designers and engineers that heat gains support the heating system in winter and external shading is a good option for the summer. This exemplary interpretation of the behavior of the South windows in the representative case shows how such information provides insights and helps domain experts to draw conclusions for design development. Besides direct engineering reasoning, sensitivities are a means to determine which parameters of a design are important. In early design phases, they provide an indicator which decisions should be made early to reduce the uncertainty in predictions and, thus, offer potential in guiding decision makers through the process [60].

The component-based structure of the model and the calculation of sensitivities makes system analysis and, especially, complexity metrics [42] available. This connects data-driven models to the approach of the design structure matrix (DSM) that deals with the structure of design artefacts, processes and teams and aims at an optimal management of dependencies [61]. As an example of such techniques, Figure 5 shows the sensitivity matrix of key variables and main internal parameters extending information shown in Figure 4. Analyzing the matrix reveals clusters, such as strong geometric dependencies at the top of the matrix, the window g-value and u-value discussed before, and a cluster of operation linking office hours, heat gain of equipment and light and occupancy to loads and energy demand (last four rows and columns of the matrix). This directs decision makers to parameter groups that need to be considered simultaneously.

Moreover, summing up columns and rows in the matrix delivers activity and passivity, which are two common metrics



of systems variables [42]. Activity (Fig. 5b) points to variables that have high potential to control the system. In the example, the matrix points to an important role of building geometry. The passivity (Fig. 5c) reveals parameters that have strong reactions and, thus, strongly depend on the configuration of the system.

Among these parameters, cooling load is striking, which means the system in its current configuration is relatively sensitive to cooling loads; there is high potential to improve performance by looking at this parameter and its influencers.

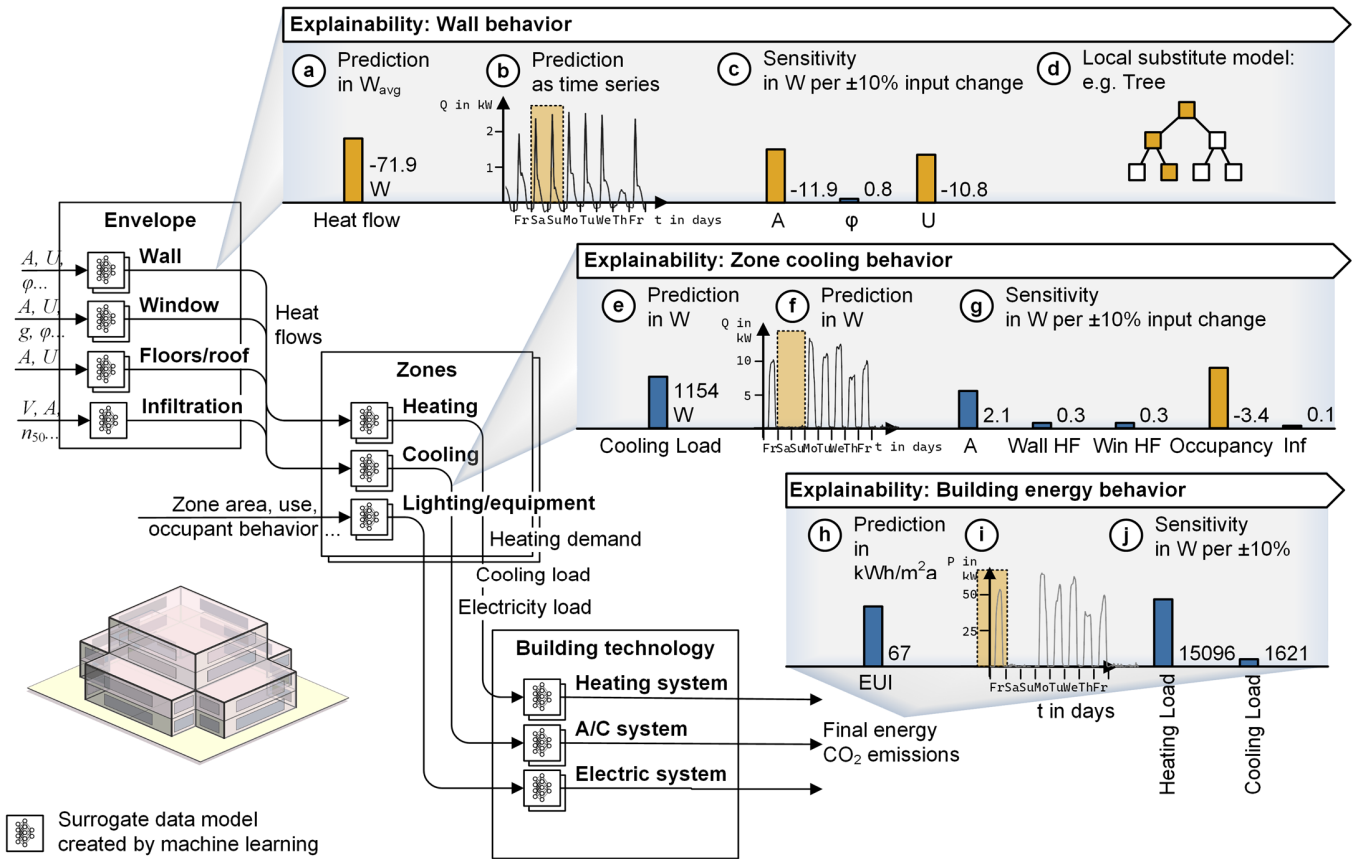


**Fig. 3. Accessing information of explainability and interpretability in a component-based machine learning model.** Accessing activations as engineering quantities with units between the components provides manifold engineering insights. The analysis of flows in averages and totals (a) (e) (h) and time series (the orange dashed box indicates the weekend) (b) (f) (i), sensitivities (c) (g) (j) and extracted rules based on decision trees (d) provides engineering insights. Humans can interpret results and understand the artefact’s behavior.

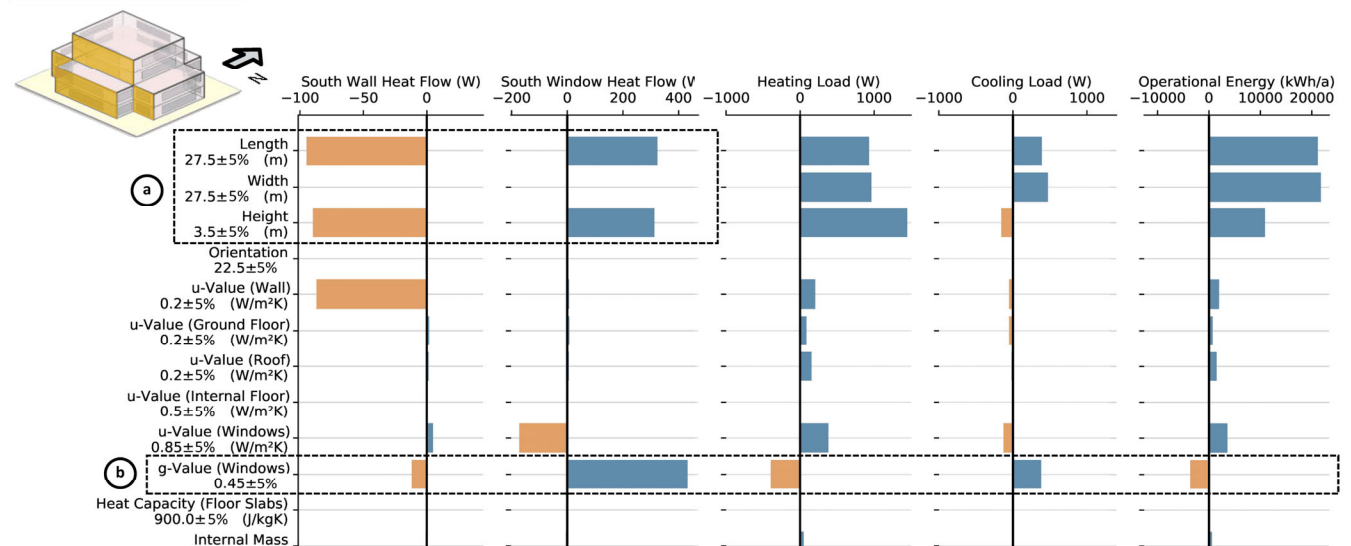




**Fig. 4. Selected sensitivities of the representative test case.** The sensitivities provide domain experts with information to identify important variables of a design configuration. **(a)** A high sensitivity to geometry and higher gains than losses through the South window are visible; **(b)** The thermal transmittance of the walls and windows (u-value) mainly influences heat losses; **(c)** The examination of the g-value allows to understand if gains happen in summer or winter in terms of heating or cooling demand; **(d)** Overall, geometry changes govern the influence on heating and cooling demand as well as total operational energy followed by the g-value of the windows.

In sum, the calculation of sensitivities as means to understand dependencies delivers valuable information on the system’s structure. This information provides decision makers with understanding of which are the key parameters to control system’s performance and prioritize parameters. The use of data-driven models and CBML allows for the quick calculation of such information. Furthermore, this information provides a plausibility check in terms of engineering by comparing dependencies to domain knowledge.

### 4.3 Rules from local decision trees

DSE data, local models, and the derivation of rules can provide further information on the systems characteristics. Figure 6 exemplifies a tree as a local model for behavior of different window options of the representative building and provides design rules related to the current configuration to control the heat and radiation passing through the windows. Examining split points allows the derivation of what-if rules as examined deeper in [62]. The initial split for the configuration is the size of windows (Fig. 6a) telling the decision maker that small windows require different strategies than large ones. The next two split points (b) identify window orientation as the second most important criterion. Focusing on the south windows following the orange prediction path, area, and g-value, which describes the solar heat gain of windows, are the key variables to control the heat flow at the next levels (c, d). In contrast, the East window splitting also includes the u-value, which points to the importance of heat conduction for this orientation. The final prediction (e) shows that orientation and g-value are the guiding variables for the performance of the South windows telling designers to pay attention to these variables at South façades. Furthermore, the upper half of the scatter plots (a, b) provides the information that area and orientation have the highest influence. In particular, increasing area and solar incidence maximize the solar gains directing designers to passive solar building design [63]. Manual studies and extensive sampling for similar climate based on energy simulation performed in other studies confirm the importance of these variables [60, 64].

From the rules of the tree and the underlying data, the application of regression is a method to derive local engineering equations. For instance, a linear regression for the heat flow through large South windows depending on area and g-value (Fig. 6f) allows decision makers not only to derive rules from the tree but also to quantitatively assess the effect of changing window size and solar transmittance on the gains and losses.

### 4.4 Evaluation of explainability

The evaluation contains two tests according to [40]: a white box test and matching with domain knowledge. First, the white box test shown in Figure 7 compares data-driven predictions and physical simulation results of heat flows and zone loads as internal explanations. The good match with simulation data proves reliability of the internal interface information of the

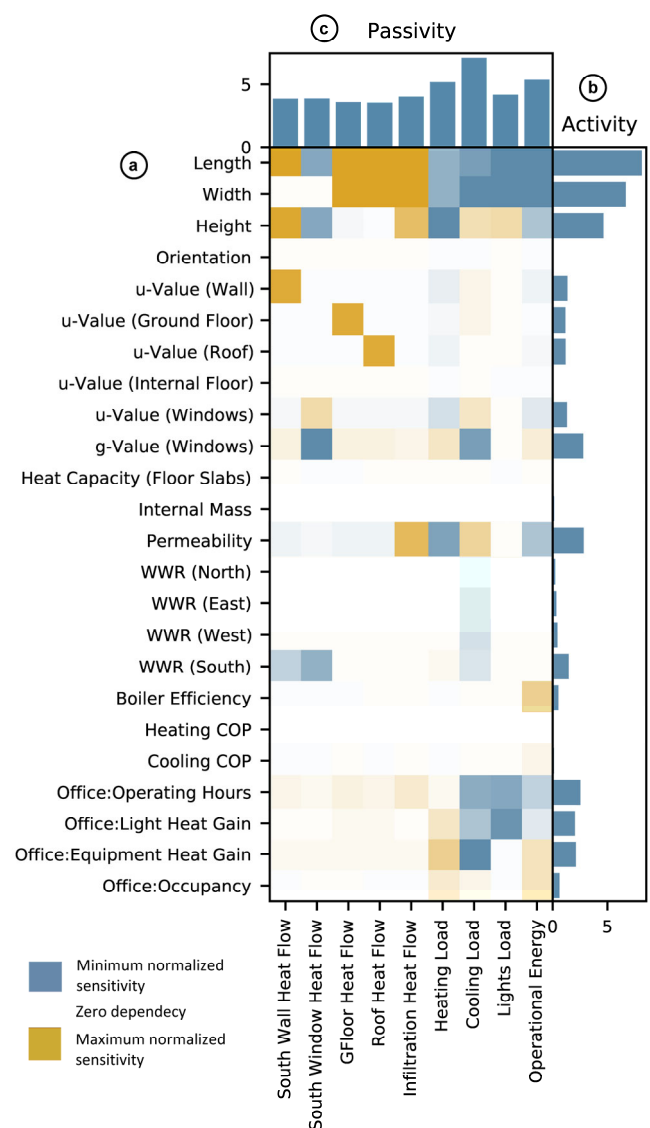


**Fig. 5. The sensitivity matrix shows dependencies between key design variables and internal parameters. (a)** The per column zero-preserving standardized sensitivities based on linear regression

coefficients show the individual dependencies between design variables and internal parameters. (b) The activity sum of absolute sensitivities determines to which extent a variable controls the outcome. (c) The passivity determines to which extent a parameter is controlled by variables.

engineers to use such numbers, e.g., to explain high or low energy consumption of a design variant and to point to causes of high local demand. Thus, the correctness of interface information is of high relevance for explainability and trust in data-driven models.

data-driven model. The reliability allows designers and

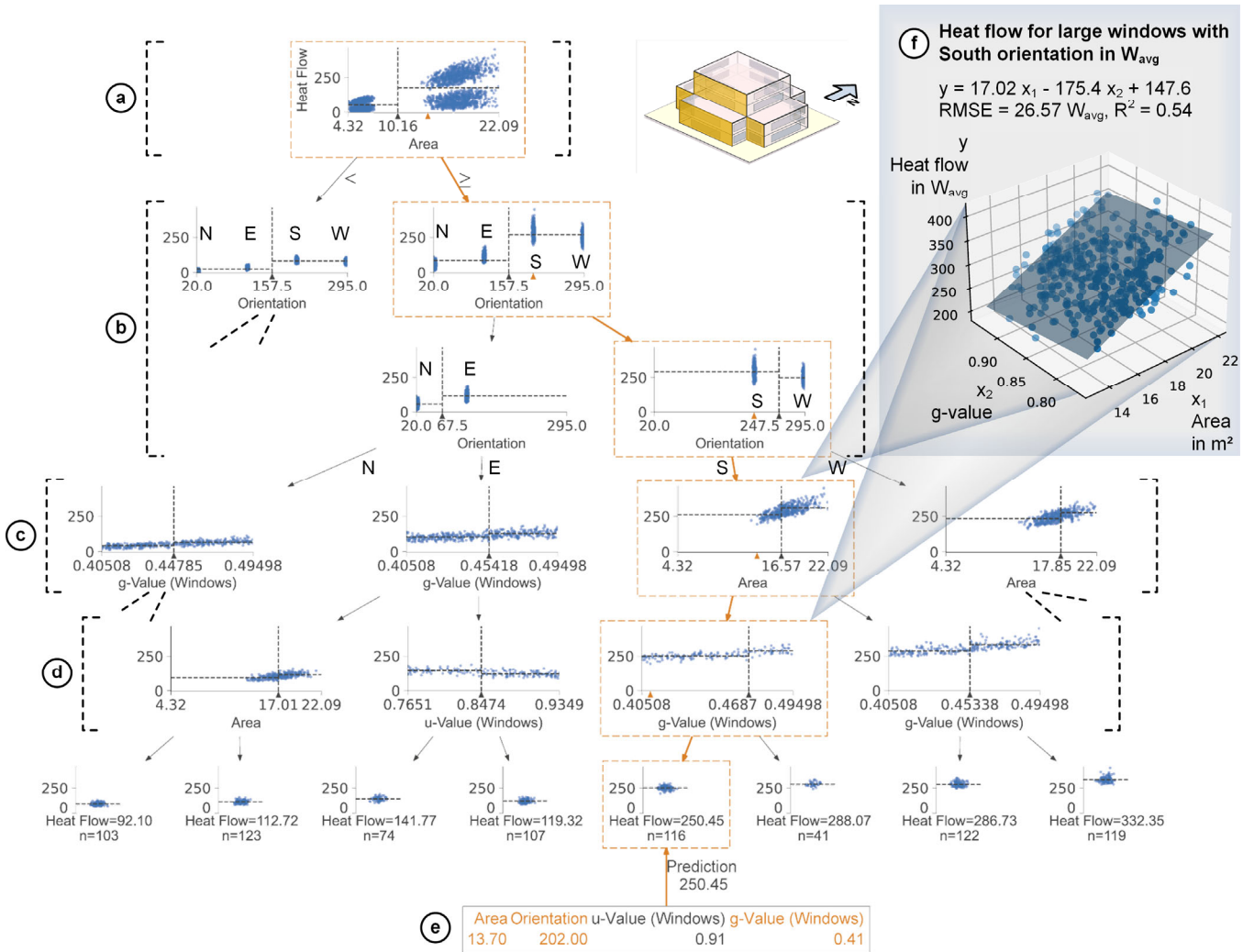


**Fig. 6. Decision tree forming a local surrogate model for the South windows.** Area (a) and orientation (b) are the most important split points. The splitting below (c, d) depends on these variables revealing specific rules for designing windows including u and g-values. This provides strategic information for the current design (e), e.g., delivered as a local surrogate model (f).

Second, we have tested if information derived from the interfaces matches domain knowledge such as described in Section 2.1 and observed in Sections 4.1 to 4.3. By examining interfaces for low energy designs (energy use intensity, EUI < 60 kWh/m<sup>2</sup>a) versus all designs, we have derived statistical the distributions at the interfaces shown in Figure 8. The interpretation of the distributions in the figure caption shows the correspondence with this domain knowledge. In summary, the strategy of large window glazing allowing sun to enter the building as well as shading for the summer relates to classical design strategy called solar passive building design that is well known in energy-efficient architecture [63]. This demonstrates

that the use of direct engineering quantities in the activations at the interfaces connects the data-driven modeling to users’ reasoning and, thus, coheres to domain knowledge provides explainability. Finally, by covering the whole design space of the representative test case, both tests cover completeness according to [40]. Finally, the presentation of simple engineering quantities delivers compactness matching the users’ context.

## 5 Discussion and Conclusions

The component-based approach of machine learning offers benefits in systems design and engineering contexts. We have demonstrated that this method provides far better generalization exploiting domain knowledge in form of structures. Creating data-driven models following decomposition schemes of the domain allows for embedding this knowledge and for representing a comprehensive range of configurations compared to conventional monolithic data-driven models limited to parametric variation. Recurring components are key to predict configurations whose structure is not included in the training data; this approach enables broader prediction context and leads to higher accuracy. Especially the two different test cases, the randomly created ones and the ones intentionally equipped with more complexity demonstrate the higher generalization capabilities ( $R^2$  of 0.94 instead of 0.71 for the feature-engineered conventional monolithic model).

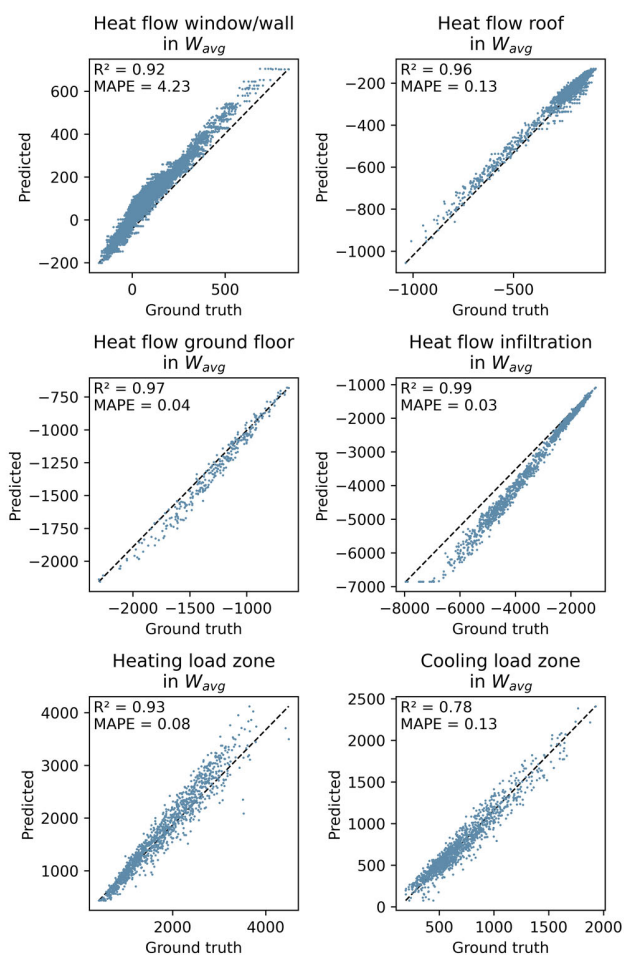


**Fig. 7. White box test comparing quantities at component interfaces.** The matching of predicted values with ground truth at component interfaces within the component system is a white box validation.

Additionally, by matching similarity in data structure and probability distribution of parameters at component level shown in Figure 1, predictions for novel design configurations differing significantly in structure become possible. Especially, the more complex manually designed representative case demonstrated that good generalization is possible when adding more complexity involving a different design structure. This reliability for an extended design space is an advantageous characteristic of the CBML method. The benefit has been proven up to now for the energy-efficient building design domain; evaluation in other domains is part of future research. Depending on similarity of domain characteristics described in Section 2.2 we expect good transferability.

The second advantage of the component-based structure is explainability. The data-driven multi-component model equals a DNN. However, at the interfaces between components, the interpretability of the activations has been demonstrated. This enables the direct understanding of parameters within the model and, thus, internal processes of the engineering artefact, as demonstrated for key quantities and flow time series in energy-efficient building design. For design activities, it is highly relevant to answer what-if questions to understand the behavior of the design artefact. Information derived from local sampling as the shown sensitivities and decision trees allows to answer such questions for specific configurations. Sensitivities provide valuable quantitative information about parameter changes directing designers and engineers to well-performing solutions. Simple trees generated for the local sampling data reveal design rules that align to the specific case. Such rules form a bridge to conventional human design and engineering knowledge and enhance it by offering quantitative case-related support. The applicability to the case and the precise configuration requires detailed examination. Hence, the use of the data-driven models has high potential to assist in the required quantitative reasoning. The component-based provides the necessary generalization and explainability of such reasoning in engineering design.

The decomposability determines the realm of applicability of the component-based method. As far as it is possible to break down a model of an artefact to interacting parts, the application of the method is possible. As such an approach is widespread in engineering design—formalized by the methods of systems engineering—there is high potential of application and integrating data-driven models with respective design activities in this way also in other fields than energy-efficient building design. Furthermore, it is relevant if the models include iterative loops. Usually, dynamic simulation serves to solve the thermodynamic behavior of buildings; By a purely hierarchical structure without any iterations, we demonstrated that it is possible to embed such dynamic behavior in a data-driven model without any iterations. The learning was able to capture the dynamic behavior, e.g. caused by storage of heat in building components and depended heat transfer to indoor space,

implicitly without the need for iteration. This demonstrates the equivalence of data-driven models to iterative solving of respective differential equations.

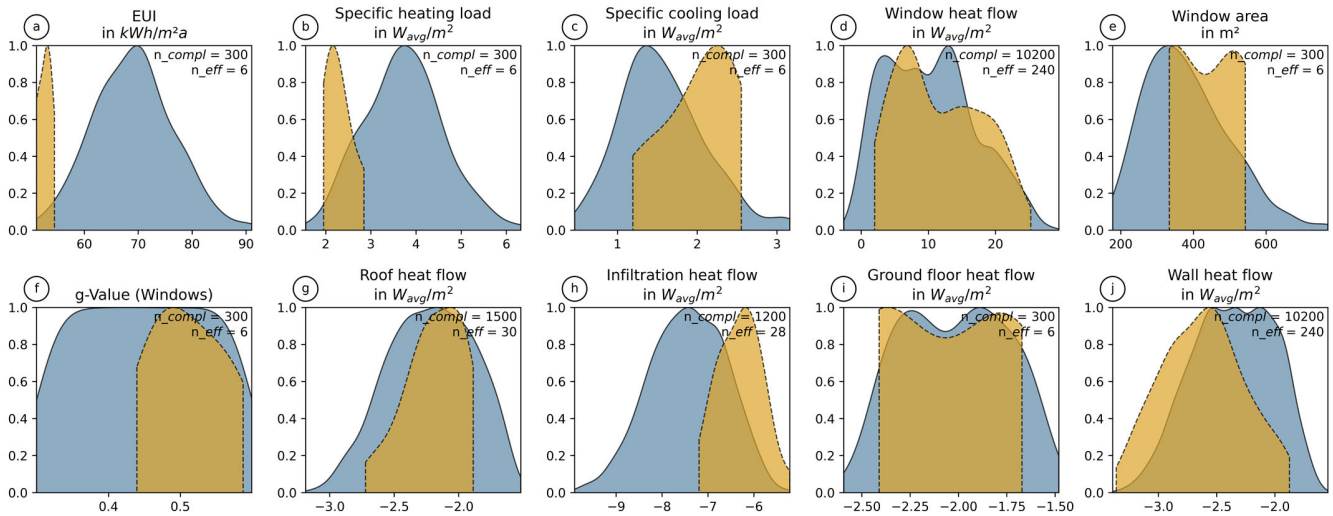


**Fig. 8. Parameter distributions of low-energy designs versus regular designs for the representative case exemplify reasonable engineering explainability at the component interfaces:** (a): The orange graphs (dashed line) show energy-efficient designs with an energy-use intensity (EUI) lower than  $55 \text{ kWh/m}^2\text{a}$  whereas the blue (solid line) shows the complete design space. (b, c): Slightly higher cooling loads by more insulation allow for significantly lower heating loads matching typical behavior of low-energy buildings. (d, e, f): This is achieved by relative high heat gains by larger windows with a high g-value on the one hand; (g, h) On the other hand, heat losses of some parts are reduced, such as the roof and infiltration of air through the envelope. (i) For ground floor heat flow, two strategies are visible, either insulation reducing heat losses in winter or less insulation allowing the building to reject heat in summer to reduce cooling loads. (j) Wall heat flows increase counterintuitively by reducing insulation; however, this is also a means to reject heat in summer and thus reduces cooling loads.

In sum, the decomposability of an engineering design by interconnected components according to the paradigm of systems engineering characterizes the applicability of component-based data-driven modelling. The advantages of generalization and explainability of the method are vital for data-driven methods to form a surrogate to replace simulation in design and engineering. On the one hand, reduced model effort and fast computation are a key to develop an intelligent assistance that supports designers and engineers in decision making with valuable information to achieve more sustainable artefacts. On the other hand, the interpretability is a valuable basis for trustworthy and responsible application of machine learning and data-driven method in engineering design.

## 6 Acknowledgements

The authors acknowledge the support of Deutsche Forschungsgemeinschaft (DFG) in form of funding the research through the grant GE1652/3-1/2 within the researcher unit FOR 2363 and through the Heisenberg grant GE1652/4-1. The computational resources and services used in this work were provided by the VSC (Flemish Supercomputer Center), funded by the Research Foundation - Flanders (FWO) and the Flemish Government – Department EWI, Belgium.

## 7 Author Contributions

**Philipp Geyer:** Conceptualization, Methodology, Software, Validation, Formal analysis, Investigation, Writing - Original draft and revisions, Visualization, Project administration, Funding acquisition

**Manav Mahan Singh:** Methodology, Software, Formal analysis, Investigation, Writing - Review & Editing + Writing Methodology, Visualization

**Xia Chen:** Methodology, Software, Formal analysis, Investigation, Writing - Review & Editing + Writing Methodology, Visualization

## 8 References

- [1] K. Amasyali and N. El-Gohary, “A review of data-driven building energy consumption prediction studies,” *Renewable and Sustainable Energy Reviews*, vol. 81, pp. 1192–1205, Jan. 2018, doi: 10.1016/j.rser.2017.04.095.
- [2] Y. Wei *et al.*, “A review of data-driven approaches for prediction and classification of building energy consumption,” *Renewable and Sustainable Energy Reviews*, vol. 82, pp. 1027–1047, Feb. 2018, doi: 10.1016/j.rser.2017.09.108.
- [3] T. Østergård, R. L. Jensen, and S. E. Maagaard, “A comparison of six metamodeling techniques applied to building



- performance simulations,” *Applied Energy*, vol. 211, pp. 89–103, Feb. 2018, doi: 10.1016/j.apenergy.2017.10.102.
- [4] L. Zhang *et al.*, “A review of machine learning in building load prediction,” *Applied Energy*, vol. 285, p. 116452, Mar. 2021, doi: 10.1016/j.apenergy.2021.116452.
- [5] S. Fathi, R. Srinivasan, A. Fenner, and S. Fathi, “Machine learning applications in urban building energy performance forecasting: A systematic review,” *Renewable and Sustainable Energy Reviews*, vol. 133, p. 110287, Nov. 2020, doi: 10.1016/j.rser.2020.110287.
- [6] P. Westermann and R. Evins, “Surrogate modelling for sustainable building design – A review,” *Energy and Buildings*, vol. 198, pp. 170–186, 2019, doi: <https://doi.org/10.1016/j.enbuild.2019.05.057>.
- [7] R. Olu-Ajayi, H. Alaka, I. Sulaimon, F. Sunmola, and S. Ajayi, “Machine learning for energy performance prediction at the design stage of buildings,” *Energy for Sustainable Development*, vol. 66, pp. 12–25, Feb. 2022, doi: 10.1016/j.esd.2021.11.002.
- [8] H. Salehi and R. Burgueño, “Emerging artificial intelligence methods in structural engineering,” *Engineering Structures*, vol. 171, pp. 170–189, 2018, doi: <https://doi.org/10.1016/j.engstruct.2018.05.084>.
- [9] H.-J. Rong, G.-B. Huang, N. Sundararajan, and P. Saratchandran, “Online Sequential Fuzzy Extreme Learning Machine for Function Approximation and Classification Problems,” *IEEE Transactions on Systems, Man, and Cybernetics, Part B (Cybernetics)*, vol. 39, no. 4, pp. 1067–1072, Aug. 2009, doi: 10.1109/TSMCB.2008.2010506.
- [10] J. Duan, Y. Ou, J. Hu, Z. Wang, S. Jin, and C. Xu, “Fast and Stable Learning of Dynamical Systems Based on Extreme Learning Machine,” *IEEE Transactions on Systems, Man, and Cybernetics: Systems*, vol. 49, no. 6, pp. 1175–1185, Jun. 2019, doi: 10.1109/TSMC.2017.2705279.
- [11] G. Huang, H. Zhou, X. Ding, and R. Zhang, “Extreme Learning Machine for Regression and Multiclass Classification,” *IEEE Transactions on Systems, Man, and Cybernetics, Part B (Cybernetics)*, vol. 42, no. 2, pp. 513–529, 2012, doi: 10.1109/TSMCB.2011.2168604.
- [12] S. L. Brunton, B. R. Noack, and P. Koumoutsakos, “Machine Learning for Fluid Mechanics,” *Annual Review of Fluid Mechanics*, vol. 52, no. 1, pp. 477–508, 2020, doi: 10.1146/annurev-fluid-010719-060214.
- [13] J. H. Lee, J. Shin, and M. J. Realf, “Machine learning: Overview of the recent progresses and implications for the process systems engineering field,” *Computers & Chemical Engineering*, vol. 114, pp. 111–121, 2018, doi: <https://doi.org/10.1016/j.compchemeng.2017.10.008>.
- [14] T. Østergård, R. L. Jensen, and S. E. Maagaard, “Early Building Design: Informed decision-making by exploring multidimensional design space using sensitivity analysis,” *Energy and Buildings*, vol. 142, pp. 8–22, May 2017, doi: 10.1016/j.enbuild.2017.02.059.
- [15] Y. Shen and Y. Pan, “BIM-supported automatic energy performance analysis for green building design using explainable machine learning and multi-objective optimization,” *Applied Energy*, vol. 333, p. 120575, Mar. 2023, doi: 10.1016/j.apenergy.2022.120575.
- [16] X. Chen and P. Geyer, “Sustainability recommendation system for process-oriented building design alternatives under multi-objective scenarios,” presented at the eg-ice Workshop, 2023.
- [17] J. P. Alves and J. N. Fidalgo, “Classification of Buildings Energetic Performance Using Artificial Immune Algorithms,” in *2019 International Conference on Smart Energy Systems and Technologies (SEST)*, Sep. 2019, pp. 1–6. doi: 10.1109/SEST.2019.8849140.
- [18] A. Schlueter, P. Geyer, and S. Cisar, “Analysis of georeferenced building data for the identification and evaluation of thermal microgrids,” *Proceedings of the IEEE*, vol. 104, no. 4, 2016, doi: 10.1109/JPROC.2016.2526118.
- [19] R. Carli, M. Dotoli, R. Pellegrino, and L. Ranieri, “A Decision Making Technique to Optimize a Buildings’ Stock Energy Efficiency,” *IEEE Transactions on Systems, Man, and Cybernetics: Systems*, vol. 47, no. 5, pp. 794–807, May 2017, doi: 10.1109/TSMC.2016.2521836.
- [20] T. Häring, R. Ahmadiyahangar, A. Rosin, and H. Biechl, “Machine Learning Approach for Flexibility Characterisation of Residential Space Heating,” in *IECON 2021 – 47th Annual Conference of the IEEE Industrial Electronics Society*, Oct. 2021, pp. 1–6. doi: 10.1109/IECON48115.2021.9589216.
- [21] M. Navarro-Cáceres, A. S. Gazafrudi, F. Prieto-Castillo, K. G. Venyagamoorthy, and J. M. Corchado, “Application of artificial immune system to domestic energy management problem,” in *2017 IEEE 17th International Conference on Ubiquitous Wireless Broadband (ICUWB)*, Sep. 2017, pp. 1–7. doi: 10.1109/ICUWB.2017.8251010.
- [22] J.-S. S. Chou and D.-K. K. Bui, “Modeling heating and cooling loads by artificial intelligence for energy-efficient building design,” *Energy and Buildings*, vol. 82, pp. 437–446, Oct. 2014, doi: 10.1016/j.enbuild.2014.07.036.
- [23] A. B. Arrieta *et al.*, “Explainable Artificial Intelligence (XAI): Concepts, taxonomies, opportunities and challenges toward responsible AI,” *Information Fusion*, vol. 58, pp. 82–115, 2020, doi: <https://doi.org/10.1016/j.inffus.2019.12.012>.
- [24] Z. Chen, F. Xiao, F. Guo, and J. Yan, “Interpretable machine learning for building energy management: A state-of-the-art review,” *Advances in Applied Energy*, vol. 9, p. 100123, Feb. 2023, doi: 10.1016/j.adapen.2023.100123.
- [25] S. Singaravel, J. Suykens, H. Janssen, and P. Geyer, “Explainable deep convolutional learning for intuitive model development by non-machine learning domain experts,” *Design Science*, vol. 6, p. e23, 2020, doi: 10.1017/dsj.2020.22.
- [26] X. Chen and P. Geyer, “Machine assistance in energy-efficient building design: A predictive framework toward dynamic interaction with human decision-making under uncertainty,” *Applied Energy*, vol. 307, p. 118240, Feb. 2022, doi: 10.1016/j.apenergy.2021.118240.
- [27] S.-I. Ao, B. B. Rieger, and M. Amouzegar, *Machine learning and systems engineering*, vol. 68. Springer Science & Business Media, 2010.
- [28] Y. S. Kim and C. S. Park, “Real-time predictive control of HVAC systems for factory building using lightweight data-driven model,” *Journal of Building Performance Simulation*, vol. 16, no. 5, pp. 507–525, Sep. 2023, doi: 10.1080/19401493.2023.2182363.
- [29] J. H. Lee, J. Shin, and M. J. Realf, “Machine learning: Overview of the recent progresses and implications for the process systems engineering field,” *Computers & Chemical Engineering*, vol. 114, pp. 111–121, Jun. 2018, doi: 10.1016/j.compchemeng.2017.10.008.
- [30] A. Kumbhar, P. G. Dhawale, S. Kumbhar, U. Patil, and P. Magdum, “A comprehensive review: Machine learning and its application in integrated power system,” *Energy Reports*, vol. 7, pp. 5467–5474, Nov. 2021, doi: 10.1016/j.egy.2021.08.133.
- [31] “Brick Schema.” Accessed: Apr. 26, 2024. [Online]. Available: <https://brickschema.org/>
- [32] J. Shi, Z. Pan, L. Jiang, and X. Zhai, “An ontology-based methodology to establish city information model of digital twin city by merging BIM, GIS and IoT,” *Advanced Engineering Informatics*, vol. 57, p. 102114, Aug. 2023, doi: 10.1016/j.aei.2023.102114.

- [33] N. M. Tomašević, M. Č. Batić, L. M. Blanes, M. M. Keane, and S. Vraneš, “Ontology-based facility data model for energy management,” *Advanced Engineering Informatics*, vol. 29, no. 4, pp. 971–984, Oct. 2015, doi: 10.1016/j.aei.2015.09.003.
- [34] D. Wolosiuk and A. Mahdavi, “Application of ontologically streamlined data for building performance analysis,” in *ECPPM 2021 - eWork and eBusiness in Architecture, Engineering and Construction*, CRC Press, 2021.
- [35] P. Zhou and N. El-Gohary, “Semantic information alignment of BIMs to computer-interpretable regulations using ontologies and deep learning,” *Advanced Engineering Informatics*, vol. 48, p. 101239, Apr. 2021, doi: 10.1016/j.aei.2020.101239.
- [36] P. Delgoshaei, M. Heidarinejad, and M. A. Austin, “Combined ontology-driven and machine learning approach to monitoring of building energy consumption,” in *2018 Building Performance Modeling Conference and SimBuild, Chicago, IL, 2018*, pp. 667–674. Accessed: Apr. 26, 2024. [Online]. Available: [https://publications.ibpsa.org/proceedings/simbuild/2018/papers/simbuild2018\\_C092.pdf](https://publications.ibpsa.org/proceedings/simbuild/2018/papers/simbuild2018_C092.pdf)
- [37] S. J. Pan and Q. Yang, “A Survey on Transfer Learning,” *IEEE Transactions on Knowledge and Data Engineering*, vol. 22, no. 10, pp. 1345–1359, 2010, doi: 10.1109/TKDE.2009.191.
- [38] K. Weiss, T. M. Khoshgoftaar, and D. Wang, “A survey of transfer learning,” *Journal of Big Data*, vol. 3, no. 1, p. 9, 2016, doi: 10.1186/s40537-016-0043-6.
- [39] R. R. Hoffman, S. T. Mueller, G. Klein, and J. Litman, “Metrics for Explainable AI: Challenges and Prospects.” arXiv, Feb. 01, 2019, doi: 10.48550/arXiv.1812.04608.
- [40] M. Nauta et al., “From Anecdotal Evidence to Quantitative Evaluation Methods: A Systematic Review on Evaluating Explainable AI.” arXiv, May 31, 2022, doi: 10.48550/arXiv.2201.08164.
- [41] R. Haberfellner, O. de Weck, E. Fricke, and S. Vössner, “Systems Engineering: Fundamentals and Applications,” 2019.
- [42] M. Kreimeyer and U. Lindemann, *Complexity metrics in engineering design*. Berlin [u.a.]: Springer, 2011. [Online]. Available: <http://d-nb.info/1010922327/04>
- [43] X. Chen and P. Geyer, “Machine assistance: A predictive framework toward dynamic interaction with human decision-making under uncertainty in energy-efficient building design,” *submitted*, 2021.
- [44] P. Geyer and S. Singaravel, “Component-based machine learning for performance prediction in building design,” *Applied Energy*, vol. 228, pp. 1439–1453, Oct. 2018, doi: 10.1016/j.apenergy.2018.07.011.
- [45] S. Singaravel, J. Suykens, and P. Geyer, “Deep-learning neural-network architectures and methods: Using component-based models in building-design energy prediction,” *Advanced Engineering Informatics*, vol. 38, pp. 81–90, Oct. 2018, doi: 10.1016/j.aei.2018.06.004.
- [46] R. Sacks, C. Eastman, G. Lee, and P. Teicholz, *BIM handbook: a guide to building information modeling for owners, designers, engineers, contractors, and facility managers*. John Wiley & Sons, 2018.
- [47] W. Samek and K.-R. Müller, “Towards Explainable Artificial Intelligence,” in *Explainable AI: Interpreting, Explaining and Visualizing Deep Learning*, W. Samek, G. Montavon, A. Vedaldi, L. K. Hansen, and K.-R. Müller, Eds., in *Lecture Notes in Computer Science*, Cham: Springer International Publishing, 2019, pp. 5–22. doi: 10.1007/978-3-030-28954-6\_1.
- [48] S. Bach, A. Binder, G. Montavon, F. Klauschen, K.-R. Müller, and W. Samek, “On Pixel-Wise Explanations for Non-Linear Classifier Decisions by Layer-Wise Relevance Propagation,” *PLOS ONE*, vol. 10, no. 7, pp. 1–46, 2015, doi: 10.1371/journal.pone.0130140.
- [49] M. T. Ribeiro, S. Singh, and C. Guestrin, “‘‘Why Should I Trust You?’’: Explaining the Predictions of Any Classifier,” in *Proceedings of the 22Nd ACM SIGKDD International Conference on Knowledge Discovery and Data Mining*, in *KDD ’16*. New York, NY, USA: ACM, 2016, pp. 1135–1144. doi: 10.1145/2939672.2939778.
- [50] M. T. Ribeiro, S. Singh, and C. Guestrin, “Model-Agnostic Interpretability of Machine Learning,” in *ICML Workshop on Human Interpretability in Machine Learning*, New York, Jun. 2016.
- [51] K. Menberg, Y. Heo, and R. Choudhary, “Sensitivity analysis methods for building energy models: Comparing computational costs and extractable information,” *Energy and Buildings*, vol. 133, pp. 433–445, Dec. 2016, doi: 10.1016/j.enbuild.2016.10.005.
- [52] S. Mohseni, N. Zarei, and E. D. Ragan, “A Multidisciplinary Survey and Framework for Design and Evaluation of Explainable AI Systems.” arXiv, Aug. 05, 2020, doi: 10.48550/arXiv.1811.11839.
- [53] L. von Rueden et al., “Informed Machine Learning – A Taxonomy and Survey of Integrating Knowledge into Learning Systems,” *IEEE Trans. Knowl. Data Eng.*, pp. 1–1, 2021, doi: 10.1109/TKDE.2021.3079836.
- [54] K. Beckh et al., “Explainable Machine Learning with Prior Knowledge: An Overview,” *arXiv:2105.10172 [cs]*, May 2021, Accessed: Dec. 29, 2021. [Online]. Available: <http://arxiv.org/abs/2105.10172>
- [55] J. Clarke, *Energy Simulation in Building Design*. Oxford: Butterworth-Heinemann, 2001. [Online]. Available: <http://www.sciencedirect.com/science/article/pii/B9780750650823500012>
- [56] U.S. Department of Energy’s (DOE), “EnergyPlus.” Accessed: Jun. 01, 2021. [Online]. Available: <https://energyplus.net/>
- [57] F. N. Najm, *Circuit Simulation*. John Wiley & Sons, 2010.
- [58] J. G. de Jalon and E. Bayo, *Kinematic and Dynamic Simulation of Multibody Systems: The Real-Time Challenge*. Springer Science & Business Media, 2012.
- [59] R. Andújar, J. Roset, and V. Kilar, “Interdisciplinary approach to numerical methods for structural dynamics,” *World applied sciences journal*, vol. 14, no. 8, pp. 1046–1053, 2011.
- [60] M. M. Singh and P. Geyer, “Information requirements for multi-level-of-development BIM using sensitivity analysis for energy performance,” *Advanced Engineering Informatics*, vol. 43, p. 101026, 2020, doi: <https://doi.org/10.1016/j.aei.2019.101026>.
- [61] S. Eppinger and T. Browning, *Design structure matrix methods and applications*. Cambridge, Mass: MIT Press, 2012.
- [62] X. Chen, J. Abualdenien, M. M. Singh, A. Borrmann, and P. Geyer, “Introducing causal inference in the energy-efficient building design process,” *Energy and Buildings*, vol. 277, p. 112583, Dec. 2022, doi: 10.1016/j.enbuild.2022.112583.
- [63] J. D. Balcomb, *Passive Solar Buildings*. MIT Press, 1992.
- [64] T. Potrč Obrecht, M. Premrov, and V. Žegarac Leskovar, “Influence of the orientation on the optimal glazing size for passive houses in different European climates (for non-cardinal directions),” *Solar Energy*, vol. 189, pp. 15–25, Sep. 2019, doi: 10.1016/j.solener.2019.07.037.
- [65] M. M. Singh, “Validation of Early Design Stage EnergyPlus Model for Office Building (one-zone-per-floor model),” Sep. 2021, doi: 10.17632/5kskbt6w2s.1.
- [66] M. M. Singh, S. Singaravel, R. Klein, and P. Geyer, “Quick energy prediction and comparison of options at the early design stage,” *Advanced Engineering Informatics*, vol. 46, p. 101185, Oct. 2020, doi: 10.1016/j.aei.2020.101185.



- [67] Passivhaus Institut, *Passive House requirements*. 2015.
- [68] Bundesministerium für Wirtschaft und Energie, “Energy Saving Ordinance (EnEV) 2014, Zweite Verordnung zur Änderung der Energieeinsparverordnung, BGBl I Seite 3951 vom 18.Nov.2013.” Accessed: May 21, 2021. [Online]. Available: <https://www.bmwi.de/Redaktion/DE/Downloads/Gesetz/zweite-verordnung-zur%20aenderung-der-energieeinsparverordnung.html>
- [69] X. Chen, M. M. Singh, and P. Geyer, “Component-based machine learning for predicting representative time-series of energy performance in building design,” presented at the 28th International Workshop on Intelligent Computing in Engineering, Berlin, 2021.
- [70] Y. Freund, R. Schapire, and N. Abe, “A short introduction to boosting,” *Journal-Japanese Society For Artificial Intelligence*, vol. 14, no. 771–780, p. 1612, 1999.
- [71] Guolin Ke *et al.*, “Lightgbm: A highly efficient gradient boosting decision tree,” *Advances in neural information processing systems*, vol. 30, pp. 3146–3154, 2017.
- [72] Guolin Ke and *et al.*, “microsoft/LightGBM.” May 24, 2021. Accessed: May 24, 2021. [Online]. Available: <https://github.com/microsoft/LightGBM>
- [73] L. Breiman, J. Friedman, C. J. Stone, and R. A. Olshen, *Classification and regression trees*. CRC press, 1984.
- [74] B. Hssina, A. Merbouha, H. Ezzikouri, and M. Erritali, “A comparative study of decision tree ID3 and C4. 5,” *International Journal of Advanced Computer Science and Applications*, vol. 4, no. 2, pp. 13–19, 2014.
- [75] F. Pedregosa *et al.*, “Scikit-learn: Machine learning in Python,” *the Journal of machine Learning research*, vol. 12, pp. 2825–2830, 2011.
- [76] P Terence Parr, Tudor Lapusan, and Prince Grover, “GitHub - parr/dtreviz: A python library for decision tree visualization and model interpretation.” Accessed: May 24, 2021. [Online]. Available: <https://github.com/parr/dtreviz>

## 9 Appendix

### 9.1 Appendix A: Data Generation Using Dynamic Energy Simulation

ML model training and testing requires a large amount of training data covering different design configurations. As it is difficult to collect such examples from real buildings, a common approach is to develop and validate a dynamic simulation model and to use it to generate synthetic data. We developed an EnergyPlus (EP) [56] simulation model for an existing office building in Munich and validated this model against data measured for two years. The building’s parameters are listed in Table 1 and floor plan is shown in Figure 9. The simulation model as been validated by comparison with the measurement from an existing building that is covered by the data: The measured total of heating and cooling energy demand is 43.97 MWh/a whereas the simulated value is 43.98 MWh/a. The simulated lighting energy demand is 21 MWh/a, for which the real data is not available. The total energy demand corresponds to 54.6 kWh/m<sup>2</sup>a. The simulation model and measured data is available on Mendeley datasets [65].

Representative key design parameters and their ranges have been selected to generate data covering design configurations. In this selection previous studies and relevant German standards served as reference [66–68]. The parameters used in this article are shown in Table 2. These parameters are selected based on their relevance for the design activity at the early design stage as known from previous examination [60].

The design parameters are sampled using Sobol scheme to generate 1000 random samples for training data. For each sample, an EP model is created and simulated. Simulation results collected as training data include average and totals as well as time-series for heat flows, loads, and energy consumption. The training data consists of box-shaped building samples (Fig. 1a), while the test dataset consists of random shapes (Fig. 1b, Test Dataset 1) and a manually designed representative shape (Fig. 1b, Test Dataset 2). Latin hypercube sampling is used to generate 300 random samples for the test dataset. Additional 300 samples are generated for the representative case. The design cases of the test and representative dataset are more complex than the training dataset. This allows for testing the generalizability of CBML approach on complex design cases.

Table 1 Parameters of the simulation model for the real building

Parameters	Unit	Value
Floor-to-floor Height	M	3.25
Number of floors	-	3
u-value (Wall)		0.18
u-value (Ground Floor)	W/m <sup>2</sup> K	0.19
u-value (Roof)		0.15
u-value (Window)		0.87
g-value		0.35
Heat Capacity (Slab)	J/kgK	800
Permeability	m <sup>3</sup> /m <sup>2</sup> h	6
Internal Mass	kJ/m <sup>2</sup> K	120
Operating Hours	H	11
Occupant Load	m <sup>2</sup> /Person	24
Light Heat Load	W/m <sup>2</sup>	6
Equipment Heat Load		12
Heating COP	-	2.8
Cooling COP		3.6
Boiler Efficiency		0.95

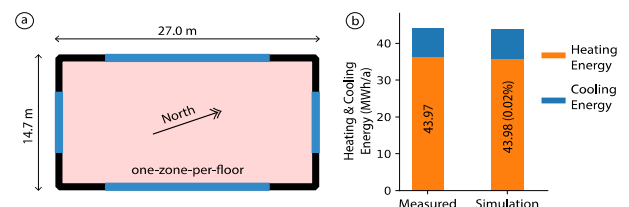


Fig. 9. Comparison of simulated and actual energy consumption. (a) building floor plan (zoning model). (b) measured and simulated heating & cooling energy requirements

### 9.2 Appendix B: Monolithic Baseline Experiment

Previously, researchers have proposed monolithic approaches to develop ML-based energy prediction model for different building shapes. This approach uses the parametric building characteristics such as area, u-values, window-to-wall ratios (WWR) etc. and shape factor or relative compactness to represent the shape characteristics. This additional feature represents the volume to façade surface ratio of the building. Using this approach, this study develops a monolithic ML model as baseline model representing best practice of data-driven modeling. The details of input features are provided in Table 3.

Table 2 Parameters and their ranges for training and test datasets

Parameter	Unit	Min	Max
Length/Width <sup>1</sup>	m	12	30
Ground Floor Area <sup>2</sup>	m <sup>2</sup>	250	800
Height	m	3	4
Orientation	Degrees	0	90
Number of Floors	-	2	5
u-value (Wall)		0.15	0.25
u-value (Ground Floor)		0.15	0.25
u-value (Roof)	W/m <sup>2</sup> K	0.15	0.25
u-value (Internal Floor)		0.4	0.6
u-value (Windows)		0.7	1.0
g-Value (Windows)	-	0.3	0.6
Heat Capacity (Slab)	J/m <sup>3</sup> K	800	1000
Internal Mass Heat Capacity	kJ/m <sup>2</sup> K	60	120
Permeability	m <sup>3</sup> /m <sup>2</sup> h	6	9
WWR <sup>3</sup>	-	0.1	0.5
Boiler Efficiency		0.92	0.98
Heating COP	-	2.5	4.5
Cooling COP		2.5	4.5
Operating Hours	h	10	12
Light Heat Gain	W/m <sup>2</sup>	6	10
Equipment Heat Gain		10	14
Occupancy	Person/m <sup>2</sup>	16	24

<sup>1</sup> Length and Width box-shaped and representative building cases

<sup>2</sup> Ground Floor Area for random shapes buildings

<sup>3</sup> Window-to-wall ratio (WWR) varies independently in each direction

The baseline monolithic ML model is trained as simple artificial neural network with one input layer, one hidden layer, and one output layer. This study uses L2 regularization and early stopping to prevent overfitting. 20% of the training samples have been used to tune hyperparameters. After a few initial runs, the learning rate has been fixed 0.001, the batch size as one-fifth of the training dataset, activation function as rectified linear unit. A total of sixteen combinations of hyperparameters (four values for number of neurons and four values for the value of regularization coefficient) have been

tried and the model with the least validation loss has been kept for further research. Table 3 shows the details of hyperparameters, used for training the monolithic ML model.

Table 3 Input and output of monolithic ML model serving as best-practice baseline

Input	Output
Floor Area (m <sup>2</sup> )	WWR [North, East, West, South] (-)
Height (m)	Operating Hours (h)
Number of Floors (-)	Light Heat Gain (W/m <sup>2</sup> )
Relative Compactness (m <sup>3</sup> /m <sup>2</sup> )	Equipment Heat Gain (W/m <sup>2</sup> )
u-value [Wall, Ground Floor, Roof, Windows] (W/m <sup>2</sup> K)	Occupancy (Person/m <sup>2</sup> )
g-Value (-)	Setpoint [Heating Cooling] (°C)
Permeability (m <sup>3</sup> /m <sup>2</sup> h)	Boiler Efficiency (-)
Internal Mass (J/m <sup>2</sup> K)	Coefficient of Performance [Heating Cooling] (-)
	Annual Energy Demand (kWh/a)

Table 4 Details of hyperparameters used for training ML components

Hyperparameter	Values
Number of Neurons	200, 400, 600, 800
Regularization Coefficient	0.0003, 0.0001, 0.00003, 0.00001
Learning Rate	0.001
Batch Size	One-fifth of sample size
Activation	Rectified Linear Unit (ReLU)

### 9.3 Appendix C: Component-Model Generation

In this approach of CBML, nine ML components are arranged in hierarchical order to predict building energy demand by use of ML for regression. The first level contains five ML components that predict heat flows, corresponding to elements and properties of the building envelope, i.e., wall, window, floor, roof, and infiltration. The second level contains three ML components that predict zone loads related to heating, cooling, and lighting. Finally, the third level has one ML component related to building systems and their properties (heating, cooling and electric) to predict building final energy demand. The input for each ML component is mentioned in Table 5.

Each ML component has a typical artificial neural network (ANN) architecture. There is one input layer, one hidden layer, and one output layer. During component training, 20% of the training data is kept as validation dataset. After few trial runs, the learning rate has been fixed to 0.001, batch size to one-fifth of the training dataset, and activation function to rectified linear unit (ReLU). The model uses both L2 regularization and early stopping to prevent overfitting. Sixteen different combinations

of coefficients for regularization and the number of neurons in the hidden layer have been tested. The best model with the least validation error has been retained for further research.

Table 5 Input and output of the ML components

ML Component	Input	Output
Wall	Area (m <sup>2</sup> ), orientation (°), u-value (W/m <sup>2</sup> K)	Heat Flow (W)
Window	Area (m <sup>2</sup> ), orientation (°), u-value (W/m <sup>2</sup> K), g-value (-)	
Floor/ roof	Area (m <sup>2</sup> ), u-value (W/m <sup>2</sup> K), heat capacity (J/kgK)	
Infiltration	Area (m <sup>2</sup> ), height (m), permeability (m <sup>3</sup> /m <sup>2</sup> h), heat capacity (J/kgK)	
Zone heating/ cooling load	Area (m <sup>2</sup> ), [wall/window/floor/ roof/infiltration], heat flow (W), Internal Mass Heat Capacity (kJ/m <sup>2</sup> K), [light/ equipment], heat gain (W/m <sup>2</sup> ), operating hours (h), occupancy (Person/m <sup>2</sup> )	Heating/ cooling Load (W)
Zone lighting load	Area (m <sup>2</sup> ), light heat gain (W/m <sup>2</sup> ), operating hours (h), window area (m <sup>2</sup> ), g-value (-)	Lighting Load (W)
Building energy demand	Boiler efficiency (-), [heating/ cooling] COP (-), [heating/ cooling/ lighting] load (W/m <sup>2</sup> )	Annual Energy Demand (kWh/a)

#### 9.4 Appendix D: Component-Model Generation for Time-Series Predictions

For time series predictors, a component also following the previously used ML-for-regression scheme has been trained and tested with an altered input/output data structure in an additional study [69]. In the data generation process, heat flow, load and energy consumption include the extra dimension time. Furthermore, time series information on the climate is included in training. Feature engineering served to extract and strengthen the periodic characteristics for the model: In our approach, timestamp formatting (year, month, week, day, day of the week, week of the month, hour, etc. plus Boolean value “is weekday”) has been applied. Another important aspect for the time series prediction is autocorrelation. Feature engineering techniques for shifting, lagging, and window averaging are usually

combined in time series data related regression or prediction tasks. In practice, for autocorrelation, input features from  $n$  previous states have been used in training phase. Depending on different periodic characteristics,  $n$  is set to 3 to 7 days or 12 to 24 hours.

Essentially, the time-series predictor is a regression model, too. The regression algorithm itself has no special requirement on tailoring to fit time series. For the balance of accuracy, difficulty of implementation and interpretability, we used the ensemble method Gradient Boosting Decision Tree (GBDT), which is developed following the concept of boosting [70]. In our implementation, LightGBM [71] using an open-source python library implementation [72] is chosen to fit the regression task.

#### 9.5 Appendix E: Sensitivity

The case representing a typical design situation has served to perform local sensitivity analysis according to Menberg et al. [51]. Its parameters are listed in Table 6. A variation  $\Delta_i$  of  $\pm 5\%$  per design parameter has been considered to calculate local sensitivities absolute means  $\mu^*$  of the Elementary Effects (EE). The sensitivities means are calculated per flow for each variable in  $\mathbf{x}$ . They have the same units as component outputs, i.e.  $W_{avg}$ ,  $W$ , and  $kWh/m^2a$ .

Table 6 Parameters for the representative case

Parameter	Unit	Mean
Length/Width	m	27.5
Height	m	3.5
Orientation	Degrees	22.5
Number of Floors	-	4
u-value (Wall)		0.2
u-value (Ground Floor)		0.2
u-value (Roof)	W/m <sup>2</sup> K	0.2
u-value (Internal Floor)		0.5
u-value (Windows)		0.85
g-Value (Windows)	-	0.45
Heat Capacity (Slab)	J/m <sup>3</sup> K	900
Internal Mass	kJ/m <sup>2</sup> K	90
Permeability	m <sup>3</sup> /m <sup>2</sup> h	7.5
WWR <sup>1</sup>	-	0.3
Boiler Efficiency		0.95
Heating COP	-	3.5
Cooling COP		3.5
Operating Hours	h	11
Light Heat Gain	W/m <sup>2</sup>	8
Equipment Heat Gain		12
Occupancy	Person/m <sup>2</sup>	20

#### 9.6 Appendix F: Decision Trees

For the local explanation modelling, we chose classification and regression trees (CART) [73] as the surrogate model and visualized the tree nodes with data distributions. As a machine

learning model based upon binary trees, the decision tree naturally offers a straightforward interpretation and rule extraction structure for model interpretation. The training captures the relationship by examining and splitting data into binary hierarchical trees of interior nodes and leaf nodes. Each leaf in the decision tree is responsible for making a specific prediction. By exhaustive search, a decision tree carves up the feature space into groups of observations that share similar target values. Each leaf represents one of these groups. The order of the tree splitting is based on the “best” decision attribute for the next node, which is usually evaluated by the information gain (entropy) [74]. As implementations, the decision tree regressor from *scikit-learn* [75] and *dtreeviz* [76] for decision tree visualization have been used. To filter out the irrelevant variation impact from the value range, a min-max scaler transforms each feature individually from the original data to a range between 0 and 1 for splitting. For engineering interpretation, this scale is reverted after tree generation so that all split points and distribution diagrams include engineering units. For rule extraction in tree interpretation, special attention is paid to the selection of splitting dependent on the previous splitting. If the following split criterion differs in terms of feature selection dependent on a previous split, this is a strong indicator that an engineering rule is underlying, such as different treatment of windows size and façade insulations dependent on orientation in the example.